

# Oil-well lightweight cement slurry for improving compressive strength and hydration rate in low-temperature conditions

Sajjad Mozaffari<sup>a,b,c</sup>, Omeid Rahmani<sup>d,e,\*</sup>, Ali Piroozian<sup>a,c</sup>, Zaman Ziabakhsh-Ganji<sup>f</sup>, Hossein Mostafavi<sup>a</sup>

<sup>a</sup> Department of Petroleum Engineering, Faculty of Petroleum and Chemical Engineering, Science and Research Branch, Islamic Azad University, Tehran 1477893855, Iran

<sup>b</sup> Young Researchers and Elite Club, Science and Research Branch, Islamic Azad University, Tehran, Iran

<sup>c</sup> Oil Exploration Operations Company (OEOC), No 234, Taleghani St., Tehran, Iran

<sup>d</sup> Department of Natural Resources Engineering and Management, School of Science and Engineering, University of Kurdistan Hewlêr (UKH), Erbil 44001, Kurdistan Region, Iraq

<sup>e</sup> Department of Petroleum Engineering, Mahabad Branch, Islamic Azad University, Mahabad 5913933137, Iran

<sup>f</sup> Faculty of Civil Engineering and Geosciences, Delft University of Technology, 2600 AA Delft, The Netherlands

## ARTICLE INFO

### Keywords:

Lightweight cement  
Conventional slurry  
Oil well  
Compressive strength  
Hydration rate

## ABSTRACT

Inadequate early compressive strength is a common problem when employing lightweight cement (LWC) slurries during the cementing of oil wells under low-temperature conditions. A new formulation of LWC slurry was investigated by the Research Institute of Petroleum Industry (RIPI) to improve the compressive strength and hydration rate of LWC slurries in low-temperature conditions. In this study, bottom-hole static temperature (BHST) ranges from 21 °C to 82 °C. Halliburton cement friction reducer (CFR-3), Litefil microspheres (D-124), hydroxy ethyl cellulose (D-112), styrene butadiene latex (D-600), and high strength hydrophobic silica (HSL-2) were as lightweight additives to make the RIPI-LWC formulation. The results showed that adding more 5 g of HSL-2 nanoparticles causes in a low-density cement slurry from 1442 kg/m<sup>3</sup> to 1281.5 kg/m<sup>3</sup>. Besides, at the temperature of 21 °C, the strength value (i.e., 3.5 MPa @ 3:56 h) was developed much faster than the temperature of 82 °C (i.e., 3.5 MPa @ 20:48 h), providing more significant insights into applying the proposed lightweight cement by reducing curing time. Furthermore, the hydraulic bonding of cement slurry was increased by attention to the action of thixotropic additive in preventing the gas migration from the cement slurry. The involvement of the new RIPI-LWC implies that cement columns can be pumped higher in the annulus, multiple-stage cementing becomes unnecessary without reducing cement integrity, and it is more economical and cost-effective than previous RIPI formulations.

## 1. Introduction

For decades, it can be challenging to place sufficient cement while drilling behind the casing without using extended low-density cement slurries or multiple-stage cementing operations [1,2]. This challenge is required considerable attention, especially in mechanically weak

formations. There is certainly no single slurry to be applied at any condition while drilling wellbores. Slurries are selected based on their potential hazards, cost, and long-term zonal isolation expectations [3–6].

Developing an adequate cement slurry compatible with underground formations at a low-temperature condition is one of the most significant

**Abbreviations:** LWC, lightweight cement; RIPI, Research Institute of Petroleum Industry; WOC, waiting-on-cement; ASTM, American Society for Testing and Materials; API, American Petroleum Institute; MSR, moderate sulfate resistance; HSR, high sulfate resistance; C<sub>3</sub>S, tricalcium silicate; C<sub>2</sub>S, dicalcium silicate; C<sub>3</sub>A, tricalcium aluminate; C<sub>4</sub>AF, tetracalcium aluminoferrite; BWOC, by weight of cement;  $\mu_a$ , apparent viscosity;  $\theta_n$ , dial reading; N, rotor standard speed;  $\mu_p$ , plastic viscosity; Y<sub>p</sub>, yield point; Ft, filtration volume; UCA, ultrasonic cement analyser; MPA, mega Pascal; BC, Bearden units of consistency; nm, nanometer; XRD, X-ray diffraction; °C, degree Celsius; mL, milliliter.

\* Corresponding author at: Department of Natural Resources Engineering and Management, School of Science and Engineering, University of Kurdistan Hewlêr (UKH), Erbil 44001, Kurdistan Region, Iraq.

E-mail address: [omeid.rahmani@ukh.edu.krd](mailto:omeid.rahmani@ukh.edu.krd) (O. Rahmani).

<https://doi.org/10.1016/j.conbuildmat.2022.129301>

Received 2 July 2022; Received in revised form 4 September 2022; Accepted 26 September 2022

Available online 8 October 2022

0950-0618/© 2022 Elsevier Ltd. All rights reserved.

factors in a successful cementing operation [7–9]. For many years, the lack of a suitable cement casing in low-temperature conditions has existed as the main challenge in oilfields. However, there has been a renewed interest in developing various types of cement composition to gain early compressive strengths in these conditions [10]. Commonly, lightweight cements (LWCs) have not well-performance in low-temperature conditions [11]. The fact that the low-temperature conditions severely retard the set of cement is well-known work in the drilling operation [12–14]. In this regard, cement hydration is an essential chemical reaction with molecular movement inhibited in which the reaction rate or hydration rate is decreased at lower temperatures. This problem is compounded in lightweight slurries wherein the reaction rates are slow, and less reactive cement per water content is available for the hydration process. Therefore, there are continuing needs for low-density cement compositions in low-temperature conditions, which have a high hydration rate, enhanced compressive strength, and low permeability upon setting for cementing pipe in wellbores. Incidentally, the principal chemical criterion for classifying Portland cement is the relative distribution of the main clinker phases known as the potential phase composition. It is established by the American Society for Testing and Materials [15] and the American Petroleum Institute (API) to promote consistency of performance among cement manufacturers.

Specifications of the API Portland well cement (API standard 10 A, 24<sup>th</sup> edition) are categorized at six classes, designated A through H (i.e., A, B, C, D, G, and H). These classes are based on the depth, temperature, and pressure in which the well cement is placed and exposed. According to Nelson and Guillot [16], in these classes, C<sub>3</sub>A (tricalcium aluminate) content indicates different degrees of sulfate resistance in cement, including ordinary (O), moderate sulfate resistance (MSR), and high sulfate resistance (HSR). Table 1 presents each API class description and its ASTM equivalent and phase composition. As given in Table 1, acceptance requirements for the fineness test are a minimum SSA (m<sup>2</sup>/kg). Classes D, G, and H cements have no fineness requirement. Also, the curing temperature is maintained at the indicated temperature for each cement class (i.e., ± 2 °C).

Despite vigorous research over the last decades [17,18], a reliable direct method for determining the concentrations of clinker phases in Portland cement has been conceptually challenging to define precisely yet. This goal is elusive because of the phases' chemical similarity. In this regard, the physical and chemical identification techniques are

generally used, such as petrographic microscopy and X-ray diffraction (XRD). The Rietveld method for powder XRD is an improved technique for determining the phase composition of Portland cement [19,20]. Through the use of derived reference diffraction patterns based on crystal structure models, this method enables standardization of powder diffraction analysis [16,21]. Besides, the most extensively used method describing the relative proportions of the major clinker phases is based on calculations on the cement's oxide composition. Taylor [22] employed more realistic phase compositions. Although other adjustments have been proposed, this employment represents a computed mineralogical composition close to the XRD results with widespread approval. Table 2 presents the equations required to calculate the potential phase composition in the cement slurry. From Table 2, chemical equilibrium is created at the clinkering temperature and maintained during the crucial cooling time, leading to incorrect outcomes [16,23].

This research proposes a feasible approach by developing a new lightweight cement (LWC) slurry with an adequate compressive strength and hydration rate in the Research Institute of Petroleum Industry (RIPI), Iran. To this aim, a new formulation of LWC slurry is investigated to improve compressive strength and hydration rate in low-temperature conditions wherein bottom-hole static temperature (BHST) ranges from 21 °C to 82 °C. From this new approach, the RIPI-LWC is proposed to provide successful zonal isolation in which the system would have been working with the conventional-density cement. The RIPI-LWC can improve the system and redesign the casing program and frequently eliminate stage-tool cementing in long intervals within the system without reducing cement integrity.

### 1.1. Conventional LWC slurries in low-temperature conditions

Conventional lightweight cements or water-extended formulations of API Class Portland cements are usually made by adding more water and sufficient material like bentonite [14,24], diatomaceous earth [25], sodium metasilicate [26], expanded perlite, gilsonite [11], and fly ash [27] to lighten the mixture and keep the solids from separating. In oil-well cement, bentonite is the most former additive utilized to reduce the slurry weight and enhance its volume [24,28], with a high availability in the study area. Bentonite is added to any API Class Portland cement in concentration from 1 to 16 wt% of the cement. Dry-mix cement (8–12 %) requires about 4.92 L of water for each 2 %

**Table 1**

Typical composition of API standard class (10 A, the 24<sup>th</sup> edition) and ASTM type cement, partially adopted from Nelson and Guillot [16].

| API (Class) | Minimum specific surface area (m <sup>2</sup> /kg) | Final curing temperature (°C) | ASTM (Type) | Intended for the use of depth (m) | Potential phase composition (wt.%) |                    |                  |                   |
|-------------|--|-------------------------------|-------------|-----------------------------------|------------------------------------|--------------------|------------------|-------------------|
|             |  |                               |             |                                   | C <sub>3</sub> S                   | β-C <sub>2</sub> S | C <sub>3</sub> A | C <sub>4</sub> AF |
| A           | 150  | 38                            | I           | 0–1830                            | 45                                 | 27                 | 11               | 8                 |
| B           | 160  | 38                            | II          | 0–1830                            | 44                                 | 31                 | 5                | 13                |
| C           | 220  | 38                            | III         | 0–1830                            | 53                                 | 19                 | 11               | 9                 |
| D           | NR   | 77                            | NA          | 1830–3050                         | 28                                 | 49                 | 4                | 12                |
| G           | NR   | 38                            | Nominal II  | 0–2440                            | 50                                 | 30                 | 5                | 12                |
| H           | NR   | 38                            | Nominal II  | 0–2440                            | 50                                 | 30                 | 5                | 12                |

C<sub>3</sub>S: tricalcium silicate; C<sub>2</sub>S: dicalcium silicate; C<sub>3</sub>A: tricalcium aluminate; C<sub>4</sub>AF: tetracalcium aluminoferrite; NR: no requirement; NA: not applicable.

**Table 2**

Equations for calculating potential phase composition in the cement slurry, adopted from Nelson and Guillot [16].

| Al <sub>2</sub> O <sub>3</sub> /Fe <sub>2</sub> O <sub>3</sub> ratio | Potential phase composition (wt. %)  |  |
|--|--------------------------------------|--|
| ≥0.64  | C <sub>3</sub> S                     | $(4.071 \times \text{CaO}) - (7.600 \times \text{SiO}_2) - (6.718 \times \text{Al}_2\text{O}_3) - (1.430 \times \text{Fe}_2\text{O}_3) - (2.852 \times \text{SO}_3)$ |
|  | β-C <sub>2</sub> S                   | $(2.867 \times \text{SiO}_2) - (0.7544 \times \text{C}_3\text{S})$   |
|  | C <sub>3</sub> A                     | $(2.650 \times \text{Al}_2\text{O}_3) - (1.692 \times \text{Fe}_2\text{O}_3)$  |
|  | C <sub>4</sub> AF                    | $3.043 \times \text{Fe}_2\text{O}_3$   |
| <0.64  | C <sub>3</sub> S                     | $(4.071 \times \text{CaO}) - (7.600 \times \text{SiO}_2) - (4.479 \times \text{Al}_2\text{O}_3) - (2.859 \times \text{Fe}_2\text{O}_3) - (2.852 \times \text{SO}_3)$ |
|  | β-C <sub>2</sub> S                   | $(2.867 \times \text{SiO}_2) - (0.7544 \times \text{C}_3\text{S})$   |
|  | C <sub>3</sub> A                     | No present   |
|  | C <sub>4</sub> AF + C <sub>2</sub> F | $(2.100 \times \text{Al}_2\text{O}_3) + (1.702 \times \text{Fe}_2\text{O}_3)$  |

If Al<sub>2</sub>O<sub>3</sub>/Fe<sub>2</sub>O<sub>3</sub> ratio is < 0.64, a C<sub>4</sub>AF + C<sub>2</sub>F (calcium aluminoferrite) solid solution is formed.

bentonite [29]. Adding 1 % of pre-hydrated bentonite affects about 3.5 % dry-mix cement [29]. In this case, dispersants reduce the cement viscosity and keep the water amount as needed. For all cement classes, the API/ISO (international organization for standardization) proposes adding 5.3 percent more water by weight of cement (BWOC) for each 1 percent bentonite [30]; however, testing is required to establish the ideal water content. It is true that with bentonite concentration, the density of cement slurry decreases, and its yield increases. Also, it has been demonstrated that the thickening time and comprehensive strength of cement are lessened by adding a surplus percent of bentonite. For instance, the compressive strength of prepared bentonite cement that barely meets the API specifications (test conditions: 12.4 MPa, 21 °C, 1869.3 kg/m<sup>3</sup>, 24 h) will be lower than that of one prepared cement having a strength of 24.13 MPa under the same test conditions [31]. Besides, the resistance of cement is lowered against the chemical attack while bentonite and water exceed. Therefore, bentonite gives a deficient compressive strength in low-temperature conditions of wells.

Moreover, the hydration of bentonite is inhibited by high calcium (Ca<sup>2+</sup>) ion concentrations in the aqueous phase of a cement slurry. When bentonite is pre-hydrated in the mixed water before adding cement, its extension efficiency improves substantially. A slurry containing 2 % pre-hydrated bentonite BWOC is comparable to one with 8 % dry-blended bentonite [32]. Compared to an identical density slurry made by dry-blended bentonite, pre-hydrated bentonite has no discernible effect on the ultimate compressive strength. In addition, conventional lightweight cement requires a considerable amount of water to mix and pump the cement slurry.

Pourmazaheri and Soltanian [33] represented four cement slurries, named RIPI-1 to RIPI-4, with an average density of ~ 1666 kg/m<sup>3</sup>. In their study, nonuniform particle size distribution (PSD) is applied to design RIPI cement slurries. They employed PSD engineering to avoid the collapse of hollow spheres and the solid constituents from contraction. Hydrophobic silica (HSL, with size of 0.1 µm and SSA of 100 m<sup>2</sup>/g), Litefill (with size of 60 to 315 µm), and Microblock (calcium silicate hydrate, with size of 0.5 µm and SSA of 21 m<sup>2</sup>/g) particles are used as additives. A main problem with their producing method of RIPI cement slurry is an operational slurry density lower than about 1318 kg/m<sup>3</sup> cannot be achieved by adding water. Another problem with this approach is that curing time or waiting-on-cement (WOC) time fails to take strength development by using nonuniform PSD in low temperatures of shallow formations. High water content plus filler materials; however, cause diminished compressive strengths. At temperatures from 21 °C to 38 °C, water-extended Portland cement is still the most common composition used in lightweight primary cementing operations. When conditions become colder, API Portland cements hydrate very slowly, and compressive strength development is severely retarded [16,34]. It is because the accurate and reliable characterization of cement slurry still presents a problem for the industry. The cement slurries exhibit a fairly complex rheological behavior, which depends not only on fluid composition and mixing procedure, but also on shear stress and temperature in testing procedure used.

Moreover, a higher surface area causes an accelerated reaction rate so that the availability of hydration sites is increased. Ai Qin et al. [35] reported that the water demand is related to SSA and packing density, in which the greater the surface area requires more water. Besides, there is a strong correlation between packing density and distribution index, and

the packing density decreases as the distribution index increases. Otherwise, the need for water increases as packing density decreases [35]. In this regard, an adequate amount of water can form a pumpable slurry, which is not much more than optimum water for cementing [36]. With the new RIPI-LWC, compressive strength can be developed more quickly by shortening the WOC time. Also, offering a well-construction solution with low permeability and low density, superior-quality cement columns can be pumped higher in the annulus, which eliminates the need for multiple-stage cementing.

## 2. Materials and methods

### 2.1. Characteristics of used additives

Halliburton cement friction reducer (CFR-3), a sulfonated resin cement dispersant (SO<sub>3</sub>:98.91 %, CaO: 0.33 %), was used to reduce the apparent viscosity and improve the rheological properties of a cement slurry in the Maroon oilfield. Using this additive, turbulent flow was achieved at lower pumping rates, which led to decrease friction pressure during pumping. Halliburton CFR-3 also helps improve fluid-loss control and provides slight slurry retardation. It is available with and without defoamer in the concentration of 0.3 to 1.5 % and 0.3 to 1.0 %, respectively (Table 3). Both products can be applied in wells above 16 °C in all API cement classes. Besides, the CFR-3 reduce hydraulic horsepower requirements and provide more significant turbulence at lower pump rates.

Furthermore, D-124 (Litefil, Schlumberger) was used to reduce cement slurry density. This reduction refers to encapsulating N<sub>2</sub> and CO<sub>2</sub> gases in D-124 microspheres, resulting in a relatively good compressive strength to cement slurry but inadequate in low-temperature conditions. D-124 microspheres are composed of 35 % Al<sub>2</sub>O<sub>3</sub> and 65 % SiO<sub>2</sub> with a space consisting of 30 % N<sub>2</sub> and 70 % CO<sub>2</sub> inside microspheres. Also, D-112 (a hydroxy ethyl cellulose) and D-600 (a styrene butadiene latex), obtained from Dowell Schlumberger, were used to prevent cement particles from settling and gas migration (gas channeling) to the cement slurry, respectively. HSL-2, high strength hydrophobic silica lightweight additive, was applied to increase the compressive strength of cement slurry in low-temperature conditions. This non-crystallized silica powder, with a size of 57 nm and surface area of 170 m<sup>2</sup>/g, was processed in IRIP and composed of micro-silicate (>65 %), Al<sub>2</sub>O<sub>3</sub>, Fe<sub>2</sub>O<sub>3</sub>, TiO<sub>2</sub>, and HCl.

### 2.2. Experimental procedure

A dry blend of lightweight additives (e.g., the first formulation with 218 g of D-124, 6 g of D-112, 113.55 cc of D-600, 4 g of CFR-3, and 2 cc of antifoam) and 1.704 kg Portland cement powder class G was mixed to 750 mL distilled water (equals 44 % mass fraction of cement class G) in a cement mixer at a speed of 4000 rpm for 15 sec. According to the API standards, the mixture was blended again at a speed of 12,000 rpm for 35 sec to make an appropriate slurry. Next, the cement slurry was poured into a mud balance to measure its density. Before any measurement, the mud balance was calibrated with pure water. A free water test was run for 2 h into the graduated tube. The free water was obtained by measuring the volume of water accumulated on the top of the cement slurry. A 500 mL graduated glassware was used to determine the free

**Table 3**

Product specifications of Halliburton CFR-3 friction reducer with and without defoamer in the Maroon oilfield.

| CFR-3 friction reducer, with defoamer, product specifications    |                                   |                              |                   |                                       |        |
|--|-----------------------------------|------------------------------|-------------------|---------------------------------------|--------|
| Part no.   | Bulk density (kg/m <sup>3</sup> ) | Form                         | Packing (kg. bag) | Specific gravity (kg/m <sup>3</sup> ) | pH     |
| 100,012,206  | 608.7                             | Red-brown solid              | 22.7              | 1160                                  | –      |
| CFR-3 friction reducer, without defoamer, product specifications |                                   |                              |                   |                                       |        |
| 100,003,653  | 608.7                             | Dark red-brown solid, powder | 22.7              | 1170                                  | 7 to 9 |

water separation in the cement slurry. In doing so, shear stress values were measured by viscometer to present the flow regime of the cement slurry. Consequently, a series of experiments were performed to obtain some properties of low-density slurry, which were crucial to achieving a slurry with zero percent free water in low-temperature conditions. These experiments were carried out according to the API standards, including compressive strength, thickening time, and fluid loss tests.

### 2.3. Rheological characterization of the new RIPI-LWC

What is known about the rheological characterization of cement slurries is primarily derived from laboratory studies. A rotational viscometer test applied in this study is one of the most practical ways to calculate the rheological properties of a cement slurry. From this way, the cement slurry was sheared at a constant rate between an inner bob and an outer rotating sleeve. By selecting an available rotor standard speed (N) in rpm and an appropriate dimension of bob and rotor to design the cement slurry, the dial reading ( $\theta_n$ ) equals the apparent viscosity ( $\mu_a$ ) of Newtonian fluids (eq. (1)).

$$\mu_a = (\theta_n/N) \times 300 \quad (1)$$

Also, the rotational viscometer was used to determine rheological parameters of non-Newtonian fluid behavior. To this aim, two parameters were required to characterize fluids that follow the Bingham plastic model: the plastic viscosity ( $\mu_p$ ) and yield point (Yp) of the fluid in cp and kg/m<sup>2</sup>, respectively. By assuming Bingham plastic model in the fluid behavior, eqs. (2) and (3) were applied to determine the rheological parameters of cement slurry.

$$\mu_p = (\theta_{300} - \theta_{100}) \times 1.5 \quad (2)$$

$$Y_p = \theta_{300} - \mu_p \quad (3)$$

Where  $\theta_{300}$  and  $\theta_{100}$  are the dial reading with the viscometer operating at 300 rpm and 100 rpm, respectively.

Furthermore, a Fann-35 viscometer was used to measure the rheological properties of the cement slurry. Patterns from API viscometer specifications for testing cement and drilling fluids were applied to design the bob and rotor range. The sample was placed in graduated glassware with a capacity of 500 mL. Also, a standard mud balance was applied to measure the weight of the slurry. A primary cementing job was first outlined to test an early compressive strength cementing in one oil well from the Maroon oilfield. Besides, fluid-loss tests were applied to measure the dehydration rate of the new RIPI-LWC slurry. The well completion was followed by cementing placement in a heated filter press cell. The pressure was ranged from 0.69 MPa to 6.9 MPa across the filtration medium with a 325-mesh screen supported by a 60-mesh screen. The filtration volume ( $F_{30}$ ) was calculated from eq. (4) during 30 min.

$$F_{30} = F_t \frac{5.477}{\sqrt{t}} \quad (4)$$

Where  $F_t$  equals the filtration volume (mL) collected at time t (min). Immediately following placement, an approval test was done to evaluate the slurry fluid loss under static conditions. No provision was made in this procedure to measure fluid loss during placement, while results of fluid-loss determinations under dynamic conditions were reported.

### 2.4. Flow properties measurement

Using rheological parameters of cement slurry, the operational factors were also computed in cementing process, including cement slurry velocity inside the casing, slurry volume for a given contact time, and time required to complete the cement process. Before mixing cement additives to the cement slurry, the three features were considered to measure flow properties. The first feature, adding too much additive to

the fluid loss cement slurry, made the slurry extremely viscous, and therefore, it was not pumpable. From the second feature, the order of mixing materials was crucial and affected the rheology of cement slurry. In the third feature, very low values of slurry yield point led to settling in the cement slurry. On the other hand, very high value of the slurry yield point mean that the slurry viscosity is exceptionally high and is not pumpable.

#### 2.4.1. Compressive strength test

The most crucial problem that the LWC slurries have in low-temperature conditions is their incapability to gain early compressive strength in these conditions. To this aim, the compressive strength of cement slurries was achieved by measuring the force to crush a 2-inch set cement cube under an unconfined compressive load. First, the crushing load was used by establishing the WOC time to predict the compressive strength of cement slurries. However, it does not entirely reflect the bond of cement slurries to the pipe or formation. Therefore, a non-destructive device using ultrasonic waves was applied to predict cement slurries' compressive strength and WOC time. An ultrasonic cement analyzer (UCA, Model 304 Fann) was used to continuously measure the compressive strength of cement versus time by working four individual units to form a cement analyzer system. The UCA was designed with a maximum operating temperature of 260 °C and pressure of 138 MPa. The cement slurry was placed in a cell under conditions that simulated downhole pressure and temperature. The cement's ultrasonic velocity was measured during the fluid state and continued to any desired point of comprehensive strength test. The results were plotted vs time to show a precise and complete record of cement slurry's initial set and strength development. It is also well-known that the fineness of Portland cement is a measure of the size of cement particles achieved in the grinding process. In turn, the finer particles of cement cause a greater surface area available for contact with water and more rapid in the hydration process. Thus, Wagner turbidimeter (H-3805, Humboldt Mfg., 120 V 60 Hz) was used to determine the fineness of Portland cement by measuring the SSA, which is based on the sedimentation velocity of cement particles suspended in kerosene solution.

#### 2.4.2. Thickening time test

A thickening time test, one of the most important factors in ensuring safe operations [37], was carried out to determine the time required to mix and pump the cement slurry under simulated wellbore temperature and pressure conditions. A high-pressure high-temperature (HPHT) consistometer (Model 290, Fann) was used to measure the thickening time and determine the consistency or pumpability of cement slurry in the Maroon oilfield. Its maximum operating temperature and pressure were 204 °C and 207 MPa, respectively. The consistency or pumpability of the cement slurry was measured in Bearden units of consistency (BC), a dimensionless quantity with no direct conversion factor to more standard units of viscosity such as the poise. The thickening time test was ended by reaching the cement slurry to a consistency of 100 BC. The elapsed time between initial application of pressure and temperature on the sample of cement slurry and occurrence of 70 BC was the thickening time for the sample at a specification test schedule.

#### 2.4.3. Fluid loss test

After completing the placement phase of cementing treatment, fluid loss tests were designed to measure the rate of fluid loss from the cement slurry. A filter press from the MUDTEST complied with the requirements of the American Petroleum Institute (API RP 13B-1) was applied to analyze characteristics of drilling fluid and cement slurry [38]. Before the fluid loss test, a filter paper was placed on the standard filtration medium in the base cap. The filter press's cell body was filled with cement slurries and closed with the base cap. A pressure of 0.69 MPa to 6.9 MPa was applied to the cell by piercing compressed air or carbon dioxide from a tank. The filtrate was driven through the filter paper and outlet in the base cap and collected by graduated cylinders. After half an

hour, the amount of discharged fluids was recorded, and the fluid loss was measured from the filter cake formed on the filter paper (see eq. (4)).

### 2.5. Rheological models

Power-law and the Bingham plastic models describe cement slurries' rheological properties over a wide range of shear rates. Although the shear stress can be underestimated at the different shear rates, the power-law model does not include a parameter to exhibit the yield stress of cement slurries. At high shear rates, the viscosity of fluids tends toward a non-zero value where it is not considered in the power-law model. In comparison, the Bingham plastic model does not suffer from this disadvantage that the power-law model underestimates the shear stress at the low and high shear rates. Nevertheless, all cement slurries are not well-described by the Bingham plastic model. Plotting the shear rate values vs shear stress indicates a definite curvature tendency of some rheological data toward the shear-rate axis. In this case, the Bingham plastic model has an opposite behavior to the power-law model in terms of overestimating the shear stress values at low and high shear rates. At the low shear rates, the wellbore's wall slippage affects the data, and therefore, it is not easy to solve this opposite behavior. Besides, at the high shear rates, there is a problem overestimating the shear stress, especially in predicting the friction pressure in pipes. Similar to the low shear rate, it may be referred to the effect of wellbore's wall slippage on the data.

## 3. Results

In this section, the results from the cement slurry tests are first presented. Then, cement rheological factors such as apparent viscosity, plastic viscosity, yield point, and density are discussed. This is important to note that the yield point of cement slurry is the leading cement rheological factor. A better understanding of fluid mechanics in the wellbore can help select pumping equipment, cement composition, and placement technique. In addition, there has been little agreement on the crucial question of why typical cement jobs were not successful and proper lightweight cement could not be obtained. In reviewing the

literature, LWC slurries were commonly used in cementing wellbores in low-temperature conditions that early compressive strength has been inadequate, as an example, it appeared in wells of the Maroon oilfield. To understand the reason of this phenomenon, three tests were conducted to investigate the primary cement job and find deficiencies to the problem of LWC slurry in low-temperature conditions. In this regard, a number of essential prerequisites were therefore considered for a successful cement job, including an accurate control of slurry density, good casing-cement bond, preventing excessive slurry's filtration loss, and adequate compressive strength of the cement slurry in low-temperature conditions. An acceptable range of fluid loss additives was added to control cement slurry density. It was also beneficial to prevent the slurry's filtration loss and shrinkage. The slurry design was based on compressive strength, thickening time, and needed fluid loss (i.e., 50 mL/30 min).

### 3.1. Cementing job analysis

Two new formulations of LWC slurries with different densities (i.e., 1281.5 and 1442 kg/m<sup>3</sup>) were tested to investigate the critical need for the field conditions. Considering the following properties of cement slurries, the results are outlined in Table 4. The primary additive used to provide an adequate compressive strength of RIPI-LWC is HSL-2 with a particle size of 57 nm and measured SSA of 170 m<sup>2</sup>/g. In the first formulation, other additives are D-124, D-112, D-600, and CFR-3. There is no free water (cc) in these cement slurries. From eqs (2) and (3), the  $\mu_p$  and YP are 7.05 cp and 0.79 kg/m<sup>2</sup>, respectively, at the cement slurry without HSL-2 particles. The density of this cement slurry is 1442 kg/m<sup>3</sup>, and its apparent viscosity range from 6.47 cp to 20 cp. By adding HSL-2 nanoparticles (10 g) to the cement slurry, the values of the  $\mu_p$  and YP will be 3.16 cp and 1.13 kg/m<sup>2</sup>, respectively.

Moreover, Figs. 1 to 3 illustrate the flow behavior of cement slurries by plotting shear rate (kg/m<sup>2</sup>) vs shear stress (rpm) in the Maroon oilfield. As seen from the results, the responses related to the rotational viscometer, which is used for measuring the rheological properties of cement slurries, are subjective due to particle migration, end effects, or slippage at the rheometer wall [39], and therefore, susceptible to recall bias. Note that untreated cement slurries have a high effective viscosity

**Table 4**  
Properties and composition of new RIPI LWC slurries in the Maroon oilfield.

| Cement slurry properties  | Shear stress (kg/m <sup>2</sup> ) at relative shear rate (rpm) |                |                |                |            |            | $\mu_p$ (cp) | YP (kg/m <sup>2</sup> ) |
|---|--|----------------|----------------|----------------|------------|------------|--------------|-------------------------|
|   | $\theta_{600}$   | $\theta_{300}$ | $\theta_{200}$ | $\theta_{100}$ | $\theta_6$ | $\theta_3$ |              |                         |
| Class G: 1.704 kg<br>Distilled water: 750 cc<br>D-124: 218 g<br>D-112: 6 g<br>D-600: 113.55 cc<br>CFR-3: 4 g<br>Antifoam: 2 cc<br>$\mu_a$ : 6.47 cp to 20 cp<br>Density: 1442 kg/m <sup>3</sup> | 12.94  | 7.84           | 5.49           | 3.14           | 0.32       | 0.2        | 7.05         | 0.79                    |
| Class G: 1.704 kg<br>Distilled water: 750 cc<br>D-124: 300 g<br>HSL-2: 10 g<br>CFR-3: 5 g<br>Antifoam: 2 cc<br>$\mu_a$ : 3.48 cp to 81 cp<br>Density: 1442 kg/m <sup>3</sup>                    | 6.96   | 4.29           | 3.26           | 2.18           | 0.86       | 0.81       | 3.16         | 1.13                    |
| Class G: 1.704 kg<br>Distilled water: 1 L<br>D-124: 400 g<br>HSL-2: 15 g<br>CFR-3: 4.5 g<br>Antifoam: 2 cc<br>$\mu_a$ : 1.91 cp to 139 cp<br>Density: 1281.5 kg/m <sup>3</sup>                  | 3.82   | 2.25           | 1.81           | 1.32           | 0.88       | 0.78       | 1.39         | 0.86                    |

$$\mu_a = (\theta_n/N) \times 300; \mu_p = (\theta_{300} - \theta_{100}) \times 1.5; Y_p = \theta_{300} - \mu_p$$

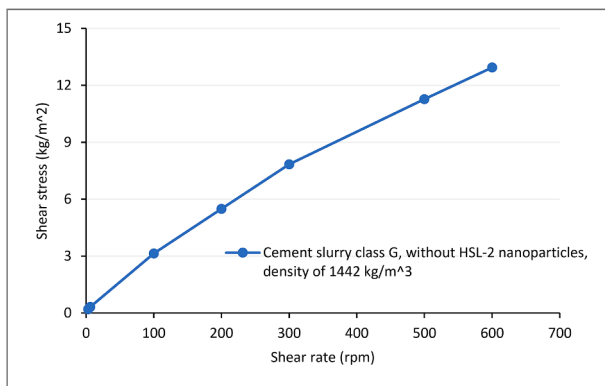


**Fig. 1.** Shear stress vs shear rates from the RIPI-LWC slurry with a density of  $1442 \text{ kg/m}^3$  in the Maroon oilfield, composed of Class G: 1.704 kg, distilled water: 750 cc, D-124: 218 g, D-112: 6 g, D-600: 113.55 cc, CFR-3: 4 g, and antifoam: 2 cc.

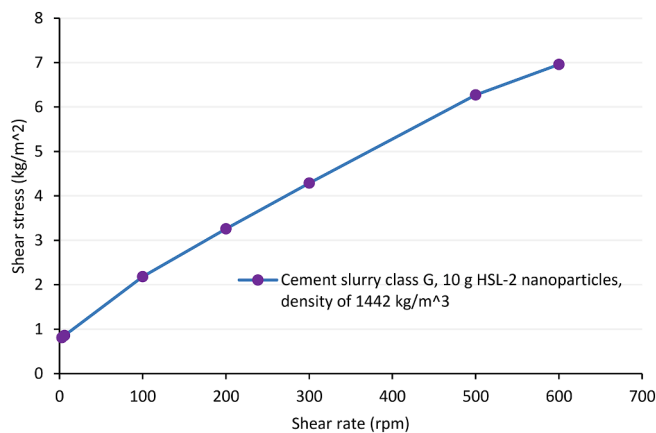


**Fig. 2.** Shear stress vs shear rates from the RIPI-LWC slurry with a density of  $1442 \text{ kg/m}^3$  in the Maroon oilfield, composed of Class G: 1.704 kg, distilled water: 750 cc, D-124: 300 g, HSL-2: 10 g, CFR-3: 5 g, and antifoam: 2 cc.

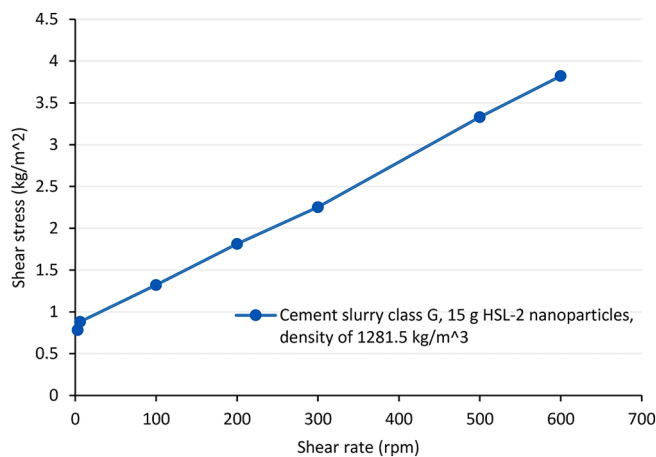


**Fig. 3.** Shear stress vs shear rates from the RIPI-LWC slurry with a density of  $1281.5 \text{ kg/m}^3$  in the Maroon oilfield, composed of Class G: 1.704 kg, distilled water: 1 L, D-124: 400 g, HSL-2: 15 g, CFR-3: 4.5 g, and antifoam: 2 cc.

at the presented shear rates during cement placement. It is desirable to reduce the effective viscosity of the slurry so that less pump horsepower will be required for cement placement. Also, there will be a reduction in the annular frictional pressure gradient and, therefore, a smaller chance

for formation fracture. Besides, the slurry can be placed in turbulent flow at a lower pumping rate. The results indicated that the drilling fluid is displaced with less mixing and less cement contamination when turbulent flow patterns.

Furthermore, shear stress of cement slurry decreases by using HSL-2 instead of D-600 and D-112, which causes the reduction of plastic viscosity of cement slurry and, thus, the annular frictional pressure gradient reduces. This reduction, in turn, results in a smaller chance of formation fracture, so this additive can act as a dispersant to reduce the viscosity (Table 4). Besides, this additive can act as a thixotropic to create rapid gelation as the slurry sets [1]. The term “thixotropic” is applied to cementing systems that achieve high gel strength in a short period if left static [40,41]. The results show that the new RIPI-LWC slurry’s gel strength is greater than the first formulation in 10 min and 10 sec. This fallback period is sufficient to prevent gas migration and circulation control loss. Also, the minimal diameter of HSL-2 particles lets them locate between the coarse grains of D-124 particles and cement powder, resulting in a decrease in the permeability of cement slurry to prevent gas migration and an increase in the compressive strength of cement slurry in low-temperature conditions.

### 3.2. Compressive strength of cement slurries

Figs. 4-6 show the UCA results of the RIPI-LWC in the BHST of 21, 38, and  $82 \text{ }^\circ\text{C}$ . From the results, the cement’s ultrasonic velocity measurements for the BHST of  $82 \text{ }^\circ\text{C}$  were started during the fluid state and continued through the initial set, 0.11 MPa @ 7:16 h, under downhole simulated pressure and temperature. The UCA then computed strength values until it reached 3.5 MPa at 20:48 h. The device’s accuracy can measure till  $\sim 138 \text{ MPa}$  of strength. After 50:28 h, the strength of the LWC slurry is 4.06 MPa. As a result, such strength value for lightweight cement in the BHST of  $82 \text{ }^\circ\text{C}$  is inadequate to overcome stresses and collapse pressures of the formation applied to cement bond during the wellbore life. Similar to the BHST of  $82 \text{ }^\circ\text{C}$ , measurements of the cement’s ultrasonic velocity for the BHST of  $38 \text{ }^\circ\text{C}$  were continued through the initial set of 0.11 MPa @ 2:16 h. The strength of set cement at the BHST of  $38 \text{ }^\circ\text{C}$  is 3.5 MPa and 7.6 MPa after 8:42 h and 53:34 h working and analyzing, respectively. Besides, in the BHST of  $21 \text{ }^\circ\text{C}$ , the initial set is 0.11 MPa @ 1:47 h. After 3:56 h and 50:28 h working and analyzing, the strength value reached 3.5 MPa and 10 MPa, respectively. Therefore, the robust formulation of RIPI-LWC in the BHST of  $21 \text{ }^\circ\text{C}$  is developed much faster than the BHST of  $82 \text{ }^\circ\text{C}$ . It can be concluded that such strength value for lightweight cement in the BHST of  $21 \text{ }^\circ\text{C}$  is perfect for overcoming stresses and collapse pressures of the formation applied to cement bond during the wellbore life.

Moreover, from Fig. 6, adding more 5 g of the HSL-2 nanoparticles can increase the compressive strength of the new RIPI-LWC slurry in lower temperatures rather than higher ones. The observed increase in the compressive strength could be attributed to the SSA of HSL-2 nanoparticles, increasing the hydration rate and early compressive strength. This combination of findings supports the conceptual premise that is an artifact of our experimental design. Besides, the results show that the achieved composition in this study is much better than the composition used by Pourmazaheri and Soltanian [33]. It is due to the fact that the time to reach the initial set (i.e., 1.47 h) is lower than previous RIPI formulations (i.e.,  $\sim 8\text{h}$ ). Hence, the WOC or curing time of the new RIPI-LWC is lower in the achieved composition, drilling operations can be started earlier, and it is more economical and cost-effective than previous RIPI formulations.

### 3.3. Thickening time and fluid loss results of new RIPI-LWC

Table 5 presents the results of permeability, porosity, thickening time, and fluid loss of the new RIPI-LWC. The selection of porosity depends on the properties sought in which the lower porosity, the shorter the thickening time, and the higher compressive strength of cement

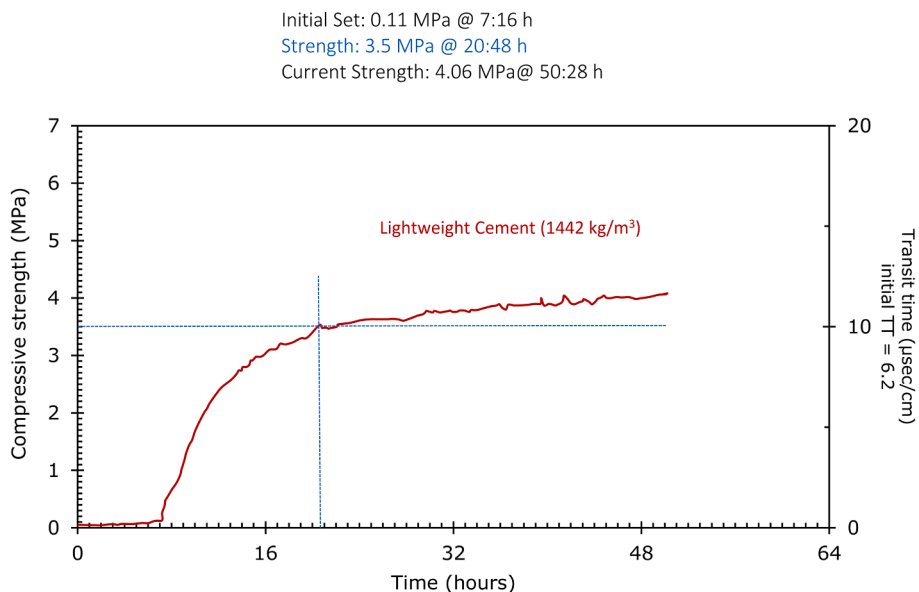


Fig. 4. The UCA results of the RIPI-LWC slurry with a density of 1442 kg/m<sup>3</sup> in the BHST of 82 °C, without HSL-2 nanoparticles.

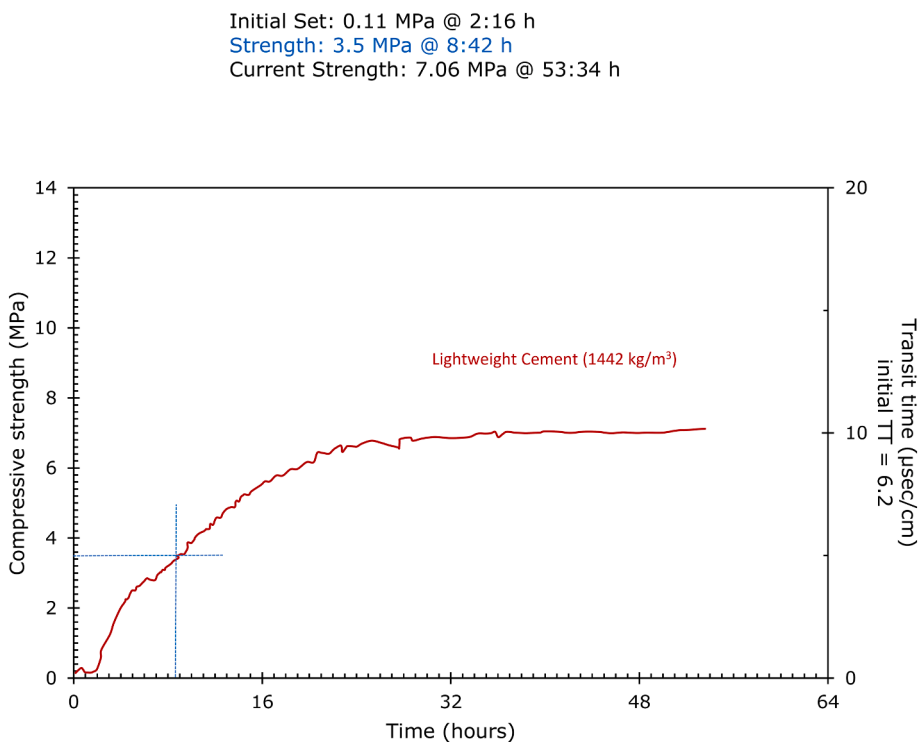


Fig. 5. The UCA results of the RIPI-LWC slurry with a density of 1442 kg/m<sup>3</sup> in the BHST of 38 °C, with 10 g HSL-2 nanoparticles.

slurry [34,42,43]. This puts more solids into cement by reducing permeability and providing greater compressive strength as well as resistance to corrosive fluids. Due to the enhanced particle size distribution ratio of the dry blend, the new RIPI-LWC slurry (i.e., permeability 0.01 mD @ 1281.5 kg/m<sup>3</sup> and 0.001 mD @ 1442 kg/m<sup>3</sup>) is more effective than the conventional RIPI slurry (i.e., permeability 0.1 mD), especially at very low porosity. During the experiment, the porosity was kept below 30 % to avoid creating a permeable matrix, and the cement

slurry in the cylindrical chamber was rotated at 150 rpm. As the apparatus introduced heat and pressure to the slurry, a continuous consistency measurement was recorded on a strip chart. The temperature and pressure of pressurized consistometer and stirred fluid loss cell equal bottom-hole circulating temperature (BHCT) and well pressure, respectively. Thickening time and fluid loss of RIPI-LWC slurries were measured with well pressure at ~ 34.5 MPa for pressurized consistometer and 3.45 MPa for stirred fluid loss cell at BHCT of 21 °C. A

Initial Set: 0.11 MPa @ 1:47 h  
 Strength: 3.5 MPa @ 3:56 h  
 Current Strength: 10.24 MPa @ 50:24 h

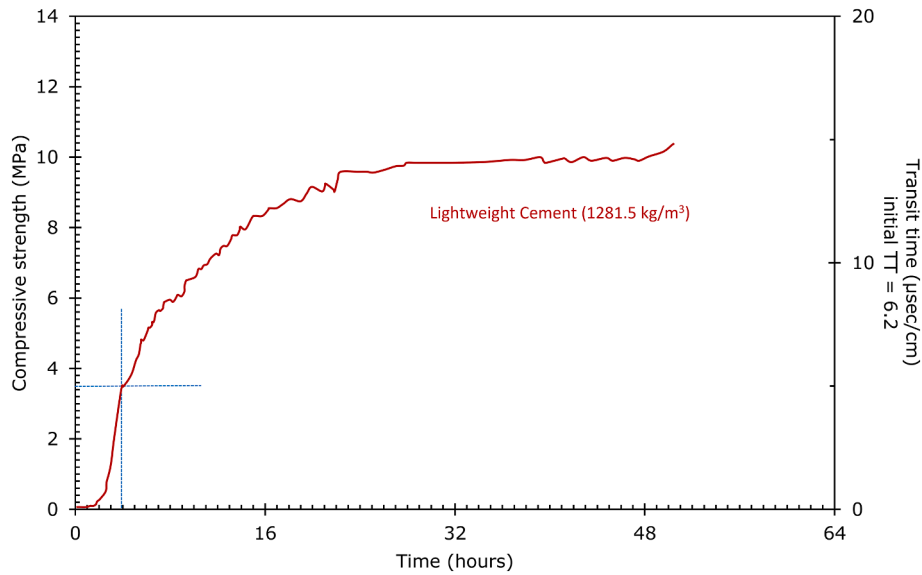


Fig. 6. The UCA results of the RIPI-LWC slurry with a density of 1442 kg/m<sup>3</sup> in the BHST of 21 °C, with 15 g HSL-2 nanoparticles.

Table 5

Thickening time and fluid loss results of the new RIPI LWC slurries.

| Properties            |           | New RIPI LWC                        |                                    |                                      |
|-----------------------|-----------|-------------------------------------|------------------------------------|--------------------------------------|
|                       |           | Density of 1281.5 kg/m <sup>3</sup> | Density of 1442 kg/m <sup>3</sup>  |                                      |
| Permeability (mD)     |           | 0.01                                | 0.001                              |                                      |
| Porosity (%)          |           | 30                                  | 30                                 |                                      |
| Heating rate          |           | PR* band (MPa)                      | Ramp time (min)                    | Soak time (min)                      |
| °F/min                | °C/min    |                                     |                                    |                                      |
| <2.0                  | <1.1      | 103.4                               | 6                                  | 6                                    |
| 2.1–3.0               | 1.16–1.65 | 103.4                               | 10                                 | 10                                   |
| 3.1–5.0               | 1.71–2.76 | 82.7                                | 35                                 | 35                                   |
| >7.0                  | >3.86     | 68.9                                | 40                                 | 40                                   |
| Thickening time (min) |           | Formulation                         |                                    |                                      |
| 30 BC                 |           | No HSL-2, 1442 kg/m <sup>3</sup>    | 10 g HSL-2, 1442 kg/m <sup>3</sup> | 15 g HSL-2, 1281.5 kg/m <sup>3</sup> |
| 70 BC                 |           | 405                                 | 90                                 | 80                                   |
| Fluid loss (cc)       |           | 420                                 | 100                                | 95                                   |
|                       |           | 125                                 | 62                                 | 70                                   |

\*PR: pressure release

pressurized consistometer was first set to measure thickening time, and then BHCT and well pressure were introduced to the slurry. The limit of pumpability was achieved when the torque on the paddle in the slurry cup reached 70 BC.

Furthermore, using the heating rate (eq. (5)) from Table 5, pressure release (PR) band, ramp time, and soak time can be determined to set the pressurized consistometer and measure the thickening time.

$$\text{Heating rate } (^\circ\text{C}/\text{min}) = \frac{\text{Difference between ambient temperature and BHCT } (^\circ\text{C})}{\text{pumping time (min)}} \quad (5)$$

For instance, in this experiment, ambient temperature and BHCT are 27 °C and 38 °C, respectively, and a pumping time of 40 min. From eq. (5), the heating rate is of 0.275 °C/min and falls within the range of <1.1

°C/min. Therefore, PR band, ramp time, and soak time are 103.4 KPa, 6 min, and 6 min, respectively. It can be seen from the data in Table 5 that the 30 BC and 70 BC thickening times of cement slurry decrease for the second formulation compared to the first formulation of RIPI-LWC slurry. Incidentally, the HSL-2 additive can act as an accelerator that causes faster reach to the consistency of 71 cp; hence, cement slurry sets too quickly and obtains high early compressive strength. It can be concluded that fluid loss of the new RIPI-LWC slurry is not high compared to other used lightweight cements.

Moreover, bonding considerations were made according to the compressive strength of cement slurries after the primary cementing operation. It was assumed that an adequate bond is provided by an additive satisfying compressive strength needed. However, field experience demonstrated that this assumption is not always applicable. According to Smith [36], two shear and hydraulic bond forces affect

cementing wellbores. Shear bond can be calculated by measuring the force needed to move a pipe in a cement casing (eq. (6)).

$$\text{Shear bond (MPa)} = \frac{\text{Force (kg)}}{\text{Contact area (m}^2\text{)}} \quad (6)$$

On the other hand, hydraulic bonding prevents fluid or gas migration in a cemented annulus. It is measured by applying pressure at the pipe/cement interface until leakage occurs [37]. Hydraulic bonding is more critical than shear bonding for zonal isolation since most cement compositions offer adequate mechanical support to hold a pipe in place. In this regard, wellbore conditions must be considered in which an optimal cement connection between pipe and formation is obtained. The new RIPI-LWC can adhere to the casing and formation face in primary cementing. Because of the high compressive strength of the new RIPI-LWC, the shear bonding increased to support the pipe in the wellbore. In general terms, this means that the effective zonal isolation increases along with the cement casing. Also, the hydraulic bonding of new IRIP-LWC increases by attention to the action of thixotropic additive in preventing the gas migration from the cement slurry.

#### 4. Conclusions

The main goal of the current study was to develop the new RIPI-LWC slurry with an adequate compressive strength and hydration rate in low-temperature conditions. The results indicated that the new formulation of RIPI-LWC in the BHST of 21 °C is developed much faster than higher temperature. The current data highlight the importance of the strength value for lightweight cement by overcoming the formation's stresses and collapse pressures applied to cement bond during the wellbore life. Also, adding more lightweight additives like HSL-2 nanoparticles can increase the compressive strength of the new RIPI-LWC slurry in lower temperatures. The observed increase in the compressive strength could be attributed to the SSA of these nanoparticles, leading to the increase in hydration rate and early compressive strength of RIPI-LWC slurry. From the cementing job analysis, shear stress of the new RIPI-LWC slurry decreases by using HSL-2 instead of D-600 and D-112 additives, which caused the reduction of plastic viscosity of cement slurry. Besides, in the achieved composition this study, the time to reach the initial set is lower than previous RIPI formulations. Therefore, the lower WOC time of the new RIPI-LWC can support earlier drilling operations with more economical and cost-effective than previous RIPI formulations.

#### CRedit authorship contribution statement

**Sajjad Mozaffari:** Writing – original draft, Conceptualization, Data curation, Resources. **Omeid Rahmani:** Investigation, Writing – review & editing, Conceptualization, Methodology. **Ali Piroozian:** Conceptualization, Methodology. **Zaman Ziabakhsh-Ganjli:** Investigation, Visualization. **Hossein Mostafavi:** Investigation, Visualization.

#### Declaration of Competing Interest

The authors declare that they have no known competing financial interests or personal relationships that could have appeared to influence the work reported in this paper.

#### Data availability

Data will be made available on request.

#### References

- [1] S. Adjei, S. Elkatatny, A.M. Abdelfattah, New lightweight cement formulation for shallow oil and gas wells, *ACS Omega* 5 (2020) 32094–32101.
- [2] A. Velayati, B. Tokhmechi, H. Soltanian, E. Kazemzadeh, Cement slurry optimization and assessment of additives according to a proposed plan, *J. Nat. Sci. Eng.* 23 (2015) 165–170.
- [3] R. Kiran, C. Teodoru, Y. Dadmohammadi, R. Nygaard, D. Wood, M. Mokhtari, S. Salehi, Identification and evaluation of well integrity and causes of failure of well integrity barriers (A review), *J. Nat. Sci. Eng.* 45 (2017) 511–526.
- [4] J. Hwang, R. Ahmed, S. Tale, S. Shah, Shear bond strength of oil well cement in carbonic acid environment, *J. CO<sub>2</sub> Utilization* 27 (2018) 60–72.
- [5] S. Huang, X. Cheng, X. Guo, Y. Shi, W. Wang, Ethanol plasma-induced polymerization of carbon fiber surface for improving mechanical properties of carbon fiber-reinforced lightweight oil well cement, *Appl. Surf. Sci.* 497 (2019), 143765.
- [6] J. Qin, X. Pang, A. Santra, G. Cheng, H. Li, Various admixtures to mitigate the long-term strength retrogression of Portland cement cured under high pressure and high temperature conditions, *Journal of Rock Mechanics and Geotechnical Engineering* (2022).
- [7] L. Soriano, J. Monzó, M. Bonilla, M. Tashima, J. Payá, M. Borrachero, Effect of pozzolans on the hydration process of portland cement cured at low temperatures, *Cem. Concr. Compos.* 42 (2013) 41–48.
- [8] C. Wang, X. Chen, R. Wang, Study on the performance and mechanism of accelerators LSA-1 and LSA-2 for deepwater well cementing at low temperatures, *J. Nat. Sci. Eng.* 32 (2016) 150–157.
- [9] Y. Bu, X. Hou, C. Wang, J. Du, Effect of colloidal nanosilica on early-age compressive strength of oil well cement stone at low temperature, *Constr. Build. Mater.* 171 (2018) 690–696.
- [10] J. Qin, X. Pang, G. Cheng, Y. Bu, H. Liu, Influences of different admixtures on the properties of oil well cement systems at HPHT conditions, *Cem. Concr. Compos.* 123 (2021), 104202.
- [11] S. Adjei, S. Elkatatny, Overview of the lightweight oil-well cement mechanical properties for shallow wells, *J. Petrol. Sci. Eng.* 198 (2021), 108201.
- [12] R.G. Da Silva Araujo, J.C.D. Filho, M.A. De Oliveira Freitas, R.M. Freitas Melo, Braga., Lightweight oil well cement slurry modified with vermiculite and colloidal silicon, *Constr. Build. Mater.* 166 (2018) 908–915.
- [13] M. Kremieniewski, Recipe of lightweight slurry with high early strength of the resultant cement sheath, *Energies* 13 (2020) 1583.
- [14] S. Adjei, S. Elkatatny, A. Al-Majed, Effect of bentonite prehydration time on the stability of lightweight oil-well cement system, *Geofluids* 9957159 (2021).
- [15] American Society for Testing and Materials, ASTM C150/C150M-20, Standard specification for Portland cement ASTM: West Conshohocken, PA, USA, 2021.
- [16] E.B. Nelson, D. Guillot, Well Cementing, Second Edition, Schlumberger, 2006.
- [17] S. Ma, D. Ge, W. Li, Y. Hu, Z. Xu, X. Shen, Reaction of Portland cement clinker with gaseous SO<sub>2</sub> to form alite-ye'elinite clinker, *Cem. Concr. Res.* 116 (2019) 299–308.
- [18] Y. Yue, J.J. Wang, P.A.M. Basheer, Y. Bai, In-situ monitoring of early hydration of clinker and Portland cement with optical fiber excitation Raman spectroscopy, *Cem. Concr. Compos.* 112 (2020), 103664.
- [19] G.L. Saouf, V. Kocaba, K. Scrivener, Application of the Rietveld method to the analysis of anhydrous cement, *Cem. Concr. Res.* 41 (2011) 133–148.
- [20] M.A.G. Aranda, Á.G.D. Torre, L.L. Reina, Rietveld quantitative phase analysis of OPC clinkers, cements and hydration products, *Rev. Mineral. Geochem.* 74 (2012) 169–209.
- [21] R.A. Young (Ed.), *The Rietveld Method*, International Union of Crystallography Monographs 5, England, Oxford University Press, Oxford, 1995.
- [22] H.F.W. Taylor, Modification of Bogue calculation, *Adv. Cem. Res.* 2 (1989) 73–77.
- [23] L.P. Aldridge, Accuracy and precision of phase analysis in Portland cement by Bogue, microscopic and X-ray diffraction methods, *Cem. Concr. Res.* 12 (1982) 381–398.
- [24] A. Samsuri, R. Junin, A.M. Osman, The utilization of Malaysian local Bentonite as an extender and free water controller in oil-well cement technology, *SPE Asia Pacific Oil and Gas Conference and Exhibition, Jakarta, Indonesia*, 2001.
- [25] T. Saidi, M. Hasan, The effect of partial replacement of cement with diatomaceous earth (DE) on the compressive strength and absorption of mortar, *Journal of King Saud University-Engineering Sciences* 34 (4) (2022) 250–259.
- [26] L. Cao, J. Guo, J. Tian, M. Hu, C. Guo, Y. Xu, M. Wang, J. Fan, The ability of sodium metasilicate pentahydrate to adjust the compatibility between synthetic Fluid Loss Additives and Retarders applying in oil well cement, *Constr. Build. Mater.* 158 (2018) 835–846.
- [27] M.U. Rehman, K. Rashid, I. Zafar, F.K. Alqahtani, M.I. Khan, Formulation and characterization of geopolymer and conventional lightweight green concrete by incorporating synthetic lightweight aggregate, *J. Build. Eng.* 31 (2020), 101363.
- [28] X. Man, A.M. Haque, B. Chen, Engineering properties and microstructure analysis of magnesium phosphate cement mortar containing bentonite clay, *Constr. Build. Mater.* 227 (2019), 116656.
- [29] S. Haney, investigation of the Effects of Bentonite in Cement-Bentonite Grouts Used for Monitor Well Completion, University, 2015.
- [30] T.M. Pique, F. Giurich, C.M. Martín, F. Spinazzola, D.G. Manzanal, Lightweight cement-based materials, Editor(s): P. Samui, D. Kim, N.R. Iyer, S. Chaudhary, *New Materials in Civil Engineering 2020*, Butterworth-Heinemann, Pages 565-589.
- [31] American Petroleum Institute (API) Spec. 10A 24<sup>th</sup> edition, Specification for Cements and Materials for Well Cementing, USA, 2015.
- [32] M. Liska, A. Wilson, J. Bensted, *Special Cements*. Editor(s): P.C. Hewlett, M. Liska, *Lea's Chemistry of Cement and Concrete (Fifth Edition)* 2019, Butterworth-Heinemann, Pages 585-640.
- [33] Y. Pourmazaheri, H. Soltanian, Application of particle size distribution engineering and nano-technology to cement recipes for some Iranian offshore oilfields, *J. Pet. Sci. Technol.* 5 (2) (2015) 70–83.
- [34] A. Anya, H. Emadi, M. Watson, An empirical model for calculating uniaxial compressive strength of oil well cements from ultrasonic pulse transit time measurements, *J. Petrol. Sci. Eng.* 183 (2019), 106387.

- [35] W. Aiqin, Z. Chengzhi, Z. Ningsheng, The theoretic analysis of the influence of the particle size distribution of cement system on the property of cement, *Cem. Concr. Res.* 29 (11) (1999) 1721–1726.
- [36] D.K. Smith, *Cementing*, Revised ed., Society of Petroleum Engineers Inc., Compliments of Halliburton Services, Richardson, TX, 1990.
- [37] K. Liu, X. Cheng, X. Zhang, X. Guo, J. Zhuang, Design of low-density cement optimized by cellulose-based fibre for oil and natural gas wells, *Powder Technol.* 338 (2018) 506–518.
- [38] American Petroleum Institute, *API RP 13B-1, Recommended practice for field testing water-based drilling fluids*, 4<sup>th</sup> Edition, 2009.
- [39] F.-J. Rubio-Hernández, Rheological behavior of fresh cement pastes, *Fluids* 3 (2018) 106.
- [40] N. Gaurina-Medimurec, B. Pašić, P. Mijić, I. Medved, Drilling fluid and cement slurry design for naturally fractured reservoirs, *Applied Sciences* 11 (2021) 767.
- [41] B. Yuan, Y. Yang, X. Tang, Y. Xie, A starting pressure prediction of thixotropic cement slurry: Theory, model and example, *J. Petrol. Sci. Eng.* 133 (2015) 108–113.
- [42] Z. Lu, X. Kong, Q. Zhang, Y. Cai, Y. Zhang, Z. Wang, B. Dong, F. Xing, Influences of styrene-acrylate latexes on cement hydration in oil well cement system at different temperatures, *Colloids Surf., A* 507 (2016) 46–57.
- [43] C. Wang, X. Chen, R. Wang, Do chlorides qualify as accelerators for the cement of deepwater oil wells at low temperature? *Constr. Build. Mater.* 133 (2017) 482–494.